J Nanopart Res (2016) 18:74
DOI 10.1007/s11051-016-3357-6

RESEARCH PAPER

Biocompatibility selenium nanoparticles with an intrinsic oxidase-like activity

Leilei Guo · Kaixun Huang · Hongmei Liu

Received: 20 September 2015 / Accepted: 3 February 2016 / Published online: 10 March 2016

Abstract Selenium nanoparticles (SeNPs) are considered to be the new selenium supplement forms with high biological activity and low toxicity; however, the molecular mechanism by which SeNPs exert the biological function is unclear. Here, we reported that biocompatibility SeNPs possessed intrinsic oxidase-like activity. Using Na_2SeO_3 as a precursor and glutathione as a reductant, biocompatibility SeNPs were synthesized by the wet chemical reduction method in the presence of bovine serum albumin (BSA). The results of structure characterization revealed that synthesized SeNPs were amorphous red elementary selenium with spherical morphology, and ranged in size from 25 to 70 nm size with a narrow distribution (41.4 ± 6.7 nm). The oxidase-like activity of the as-synthesized SeNPs was tested with 3,3′,5,5′-tetramethylbenzidine (TMB) as a substrate. The results indicated that SeNPs could catalyze the oxidization of TMB by dissolved oxygen. These SeNPs showed an optimum catalytic activity at pH 4 and 30 °C, and the oxidase-like activity was higher as the concentration of SeNPs increased and the size of SeNPs decreased. The Michaelis constant (K_m) values and maximal reaction velocity (V_{max}) of the SeNPs for TMB oxidation were 0.0083 mol/L and 3.042 μmol/L min, respectively.

Keywords Selenium nanoparticles · Oxidase-like · TMB · Biocompatibility · Biomedicine

L. Guo · K. Huang · H. Liu (✉)
School of Chemistry and Chemical Engineering, Huazhong University of Science and Technology, Wuhan 430074, People's Republic of China
e-mail: hmliu2004@126.com

Introduction

The research on nanozyme which is a novel enzyme mimic based on nanomaterial is becoming a rapidly emerging field, since ferromagnetic nanoparticles with intrinsic peroxidase-like activity were first reported in 2007 (Gao et al. 2007; Wei and Wang 2013). Various nanostructures have been reported to be enzyme-like properties. These materials include peroxidase-like activity of FeSe, CuO nanoparticles, V_2O_5 nanowires, graphene oxide, and metal nanostructures; oxidase-like activity of CeO_2, $CoFe_2O_4$, Co_3O_4 nanoparticles; peroxidase-like or oxidase-like activity of Au, Pt, and alloy nanoparticle (Dutta et al. 2012; Feng et al. 2015; Hayat et al. 2015; Lin et al. 2014; Shen et al. 2015; Zhang et al. 2013). As compared with nature enzyme, these nanostructures mimic enzyme with advantages of high stability against denaturing, excellent catalytic performance, together with easy synthesis and store in low cost. Thus, these mimic enzymes can supersede the nature enzyme using in many fields such as biosensor, colorimetric detection, immunoassays,

cancer diagnostics and therapy, and pollutant degradation.

The biological application of nanozyme has attracted a lot of attention in recent researches. For example, An et al. found that Fe_3O_4@carbon hybrid nanoparticles enhanced the ascorbic acid-induced oxidative stress and selective damage to PC-3 prostate cancer cells owing to the peroxidase mimic to create highly toxic ·OH radicals (An et al. 2013). Xu et al. reported a drug delivery using CeO_2 nanoparticles capped mesoporous silica nanoparticles (MSN)-decorated ferrocene. The intrinsic oxidase-like activity of CeO_2 could oxidize ferrocenyl moieties, which triggered the uncapping of the CeO_2 and caused the drug release (Xu et al. 2013). Gao et al. constructed peptide-AuNPs with the intrinsic peroxidase-like activity as novel nanoprobes for early cancer diagnosis and efficient treatment (Gao et al. 2015). Asati et al. expounded a new method for sensitive fluorigenic detection of cancer biomarkers at neutral pH based on the oxidase-like activity of CeO_2 nanoparticles (Asati et al. 2011). However, though many nanostructures mimic enzyme can replace the nature enzyme using in biological fields, there were little attention on the biocompatibility and toxicity of these inorganic materials. Therefore, modifying these nanozymes and discovering new nanozymes with better biocompatibility may broaden the applications of the nanozymes in biological filed.

Selenium (Se) is an essential trace element of fundamental importance to human health. Severe selenium deficiency can have adverse consequences for susceptibility to multiple diseases, including cardiovascular disease, cancer, HIV infection, Keshan disease, and Kashin-Beck disease, while selenium supplementation can protect against these diseases in humans. The biologic function of selenium is primarily implemented through its incorporation into selenoproteins containing selenocysteine, the 21st genetically encoded protein amino acid. Selenium, as well as many selenoproteins, such as glutathione peroxidase (the most abundant selenoprotein), thioredoxin reductases, is involved in antioxidant defense and the regulation of cellular redox signaling (Hatfield et al. 2014). However, the narrow margin between the nutrient and toxicity dosage of Se tremendously inhibits its application. Studies showed that the efficient dose (200 μg/day) of Se as the anticancer agent was close to or even above the toxicity range, which could cause damage to normal tissues and cells. Traditional Se compounds as inorganic and organic selenium forms containing selenite, selenomethionine (SeMet), etc., are inefficient due to their low activity and inadequate toxicity (Abdulah et al. 2005). As the forms and dose are significance for the biological function of Se, searching for novel Se species that are more effective and less toxic is an effective way to expand the application of Se. In the recent years, selenium nanoparticles (SeNPs), the red zero valent selenium, have garnered a great deal of attention as potential chemopreventive agent (Feng et al. 2014; Peng et al. 2007; Wang et al. 2014, 2015; Zheng et al. 2015), due to their excellent biological activities and low toxicity. Abundant evidence actually supports the better biocompatibility and bioefficacy of SeNPs when comparing to traditional inorganic and organic Se forms (Benko et al. 2012; Forootanfar et al. 2014; Gao et al. 2014; Huang et al. 2003; Wang et al. 2007). For example, Wang et al. revealed that SeNPs could equally increase the activities of glutathione peroxidase and thioredoxin reductase but have much lower toxicity compared with selenomethionine(Wang et al. 2007). Benko et al. showed that the toxicity of Se species decreased in the following order: selenate > selenite > SeNPs (Benko et al. 2012). Huang et al. reported that SeNPs exhibited better scavenging effects of free radicals than other Se sources, and also showed protective effects against the oxidation of DNA with low toxicity and acceptable bioavailability (Huang et al. 2003). Furthermore, SeNPs were found to be mainly concentrated in cancer cells, and such a favorable selective distribution resulted in strong proliferation suppression on cancer cells without perceived host toxicity (Wang et al. 2014). Although SeNPs has been considered as high biological activity and low toxicity, there were lack of the molecular explanation involved in their unique biological function, especially from the point of enzyme mimic even Se atoms were the active sites of selenoenzymes.

In this work, biocompatibility SeNPs were prepared and characterized by transmission electron microscopy (TEM), X-ray powder diffraction (XRD), dynamic light scattering (DLS), X-ray photoelectron spectroscopy (XPS), UV–Vis absorption, and infrared spectrum (IR). Then oxidase-like activity of the as-synthesized SeNPs was studied with the oxidization of 3,3′,5,5′-tetramethylbenzidine (TMB) by dissolved oxygen. We found for the first time that SeNPs had

intrinsic oxidase-like activity, which provided a new molecular explanation for the biological function of SeNPs observed in cell and animal experiment. Furthermore, the oxidase-like activity of SeNPs may also broaden its applications in biosensor, biochemistry detection, and other biological fields.

Experimental section

Materials

All chemicals were of analytical grade and used without further purification. Ethanol, acetic acid, sodium hydroxide (NaOH), glutathione (GSH), and sodium selenite (Na_2SeO_3) were purchased from Sinopharm Chemical Reagent Co., Ltd (Shanghai, China). Bovine serum albumin (BSA) was purchased from Biosharp (Hefei, China) and TMB was purchased from Aladdin (Shanghai, China). Double-distilled water was used throughout the whole experiment.

Preparation of the SeNPs

Colloidal SeNPs were prepared by a modified process according to the literature (Li et al. 2008). First, 5 mL of 10 mmol/L Na_2SeO_3 was mixed with 400 mg BSA under vigorous stirring, and 20 mL of 10 mmol/L GSH was added into the mixture. The color of the mixture turned into orange-red after 130 μL of 1 mol/L NaOH was rapidly injected, which indicated that the SeNPs were formed. Then, the colloidal was dialyzed using dialysis bag (MW cutoff 3500) against double-distilled water for 48 h with the water changing every 24 h to separate the oxidized glutathione (GSSG). Finally, the obtained solution was then centrifuged to abandon the suspension, while the red precipitate was dispersed into distilled water and stored at 4 °C. SeNPs with different sizes can be synthesized by adding different amounts of BSA into the redox system.

Characterization of the SeNPs

The as-obtained SeNPs were characterized by TEM, XRD, DLS, XPS, IR, and UV–Vis absorption. TEM sample was prepared by placing a drop of the colloidal dispersion onto a copper grid coated with a perforated carbon film, followed by evaporating the solvent at room temperature. Then, the TEM graphs were obtained on a Tecnai (G2 20, FEI Co., Netherlands) at an acceleration voltage of 200 kV. The average particle size and the distribution were determined from about 200 particles of the enlarged micrographs. The mean hydrodynamic diameter of SeNPs in aqueous solution was obtained using a DLS instrument (LB-550, Horiba, Ltd. Japan). XRD patterns were recorded on an X-ray diffractometer (X'Pert PRO, PANalytical B.V., Netherlands) using Cu Ka radiation with 40 kV and 55 mA in the 2θ range 10°–90°. The XPS sample was prepared by spreading the colloidal ethanol dispersion on a glass plate and dried under room temperature, and the XPS pattern was operated on an Axis-ultra Dld-600 W (Kratos, Japan) photoelectron spectrometer. IR spectra of the samples were recorded on IR spectrometer (Equinox 55, Bruker Optics, Germany) in the range of 4000–500 cm^{-1} using the KBr-disk method. UV–Vis absorption spectra were collected on a UV–Vis spectrophotometer (Shimadzu UV-2550) in the wavelength range of 190–900 nm.

Oxidase-like activity of SeNPs and kinetic studies

To investigate the oxidase-like activity of the as-synthesized SeNPs, the catalytic oxidation of the peroxidase substrate TMB in the absence of H_2O_2 was tested. In a typical experiment, 100 μL of SeNPs (60 μg/mL) dispersion was added to 3.7 mL of NaAc buffer solution (0.2 mol/L, pH 4.0) containing TMB with a series concentration at 30 °C. As the reaction proceeded during an hour, the blue color product of oxTMB was monitored in time scan mode at 652 nm using a Shimadzu UV-2450 spectrophotometer at an interval of 10 min (Gao et al. 2007). The apparent kinetic parameters were calculated based on the Michaelis–Menten equation $V = V_{max} * [S]/(K_m + [S])$, where V is the initial velocity, V_{max} is the maximal reaction velocity, $[S]$ is the concentration of substrate, and K_m is the Michaelis constant. To explore the optimal conditions of the oxidation of TMB with SeNPs, a range of temperatures (20–60 °C) and a range of pH values (3–5) for the reaction were measured under the same concentration mentioned above. To investigate the effect of the SeNPs concentration, catalytic reactions were performed in working solutions (pH 4.0 NaAc buffer, temperature 30 °C, 833 μmol/L TMB) with different concentrations of

SeNPs. To investigate the effect of SeNPs with different sizes, catalytic reactions were performed in working solutions (pH 4.0 NaAc buffer, temperature 30 °C, 833μmol/L TMB) using SeNPs with mean diameters of 38.7 nm and 55.8 nm, respectively.

Results and discussion

Characterization of the SeNPs

The morphology and size distribution of the SeNPs were characterized by TEM and DLS. As shown in Fig. 1a, the morphology of the most SeNPs was spherical-like with average size of about 38.7 nm. DLS measurement showed that SeNPs had a diameter in the range of 25–70 nm with the mean size of 41.4 nm, and the cumulative distribution under 50 nm reached to 94.9 %, which showed the formation of SeNPs with the nearly narrow size distribution (SD = 6.7 nm). TEM and DLS measurements revealed the consistent data of the average size and size distribution of the SeNPs.

There are two kind forms of element Se, Trigonal selenium (t-Se) with the gray color was known as excellent photoelectric, catalytic, and semiconducting materials; the other is amorphous (a-Se) selenium with red color (Kumar et al. 2014). Since the red SeNPs was found in the metabolites of the microorganism, the amorphous selenium, especially nano-selenium had attracted a lot attention due to their low toxicity and high utilization in the organism compared with the conventional selenium (Hunter and Manter 2009). Figure 1c shows a typical XRD pattern of the SeNPs. There were no sharp Bragg reflections except for a broad peak at the 2θ angles of 20°–30°, indicating that the as-synthesized product was amorphous Se. The XPS result of the sample revealed that the 3d orbit binding energy of SeNPs was about 55.3 eV (Fig. 1d), and these data were consistent with the standard value of element Se, which confirmed the as-prepared SeNPs was composed of element Se.

The UV–Vis absorption spectrum of SeNPs is displayed in Fig. 2a. UV–Vis absorption spectrum did not show any clear maximum in the wavelength region studied, and absorbance increases toward higher energy due to formation and surface plasmon vibration of SeNPs (Vekariya et al. 2012; Yu et al. 2015). The UV–Vis absorption spectrum of SeNPs was in accord with the orange-red color of SeNPs colloid (the inset

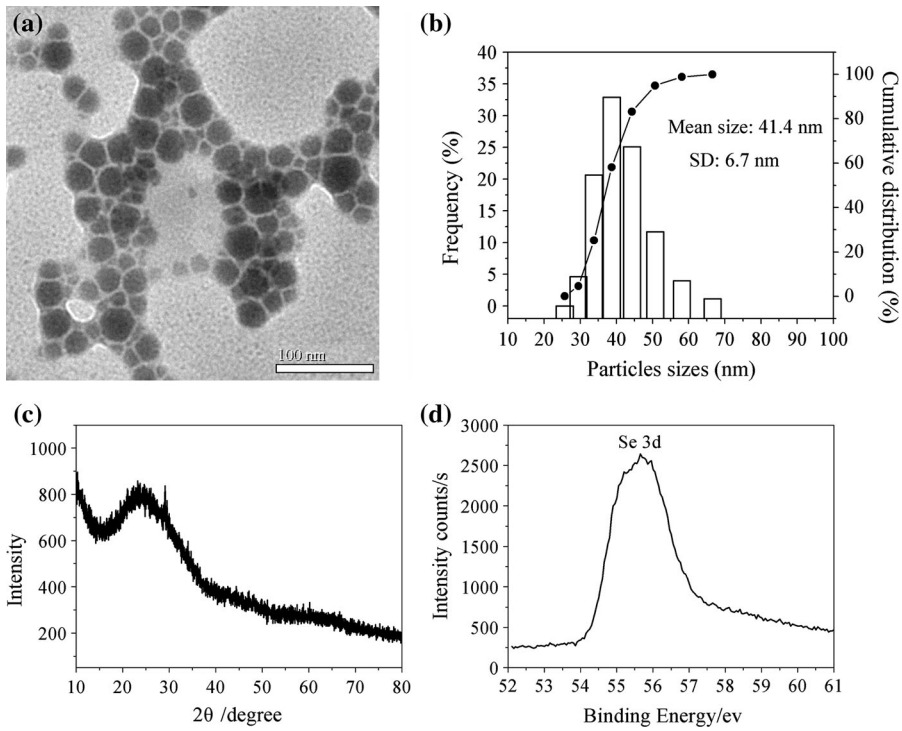

Fig. 1 **a** TEM image of the SeNPs; **b** Particle size distribution of SeNPs with DLS measurement; **c** XRD pattern of the SeNPs; **d** XPS spectrum of the SeNPs

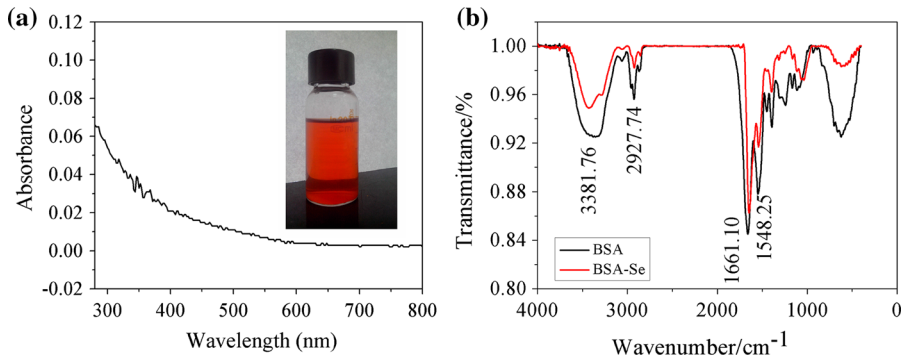

Fig. 2 **a** UV–Vis absorption spectrum of SeNPs. *Inset* showing photograph of the as-synthesized SeNPs colloid; **b** IR spectrum of the pure BSA and BSA-Se nanoparticles

of Fig. 2a). The stability of the nanoparticles is a major factor affecting its application. In order to further verify the role of BSA in the stability of the nanoparticles, IR spectra of pure BSA and BSA-Se nanoparticles are compared in Fig. 2b. In pure BSA, the characteristic vibrations of the –OH stretch, N–H stretch, and the C=O stretch in amide I were found to occur at 3381, 2927, and 1661 cm^{-1}, respectively. The IR spectra of the BSA-Se nanoparticles revealed the obvious shift of the –OH stretch, N–H stretch, and C=O stretch in amide I of the BSA, which indicated a change of the secondary structure of the BSA with SeNPs. This result confirmed that the SeNPs were stabilized by BSA through the strong interaction between the –OH, N–H and amide I with element Se.

The oxidase-like activity of the SeNPs

It was found that the substrate TMB of the peroxidase can produce a blue color slowly under the NaAc buffer in the absence of H_2O_2, which inspired us to explore whether this reaction can be accelerated by SeNPs. As shown in Fig. 3a, SeNPs could catalyze the oxidation of TMB in NaAc buffer and produce the typical color reaction during 60 min. To the contrast, the TMB-NaAc solution without SeNPs maintains colorless. Similar to other nanomaterials of enzyme mimic reactions, the maximum absorbance peak of the oxidation products of TMB (oxTMB) is located at 652 nm (Gao et al. 2007). As shown in Fig. 3b, the absorbance of the oxTMB at 652 nm was gradually increased in the presence of SeNPs (60 μg/mL) as reaction time extended, while the absorbance of the reaction system without SeNPs nearly unchanged. Figure 3c shows the UV–Vis absorption spectrum of the TMB solutions. The absorbance of TMB solutions had no absorbance peak at 652 nm before reaction. After oxidation for 60 min by dissolved oxygen without SeNPs catalyst, the TMB solutions (0.2 M NaAc, pH 4.0) at 652 nm showed a weak absorption peak, indicating the minor oxidation of TMB under this condition. The absorbance of the oxidized product of TMB at 652 nm was significantly increased in the presence of SeNPs, suggesting the obvious oxidation of TMB. These results revealed that the as-synthesized SeNPs exhibited intrinsic oxidase-like activity to the certain degree. As a commonly used peroxidase substrate, TMB is colorless and can be oxidized slowly by H_2O_2 or dissolved oxygen. The reaction mechanism may be the electron transfer from the substrate TMB to the H_2O_2 or dissolved oxygen, and the oxidation of TMB can be accelerated in the presence of the enzyme or catalyst. Figure 3d shows the UV–Vis absorption spectra of SeNPs before and after catalyzing the oxidation of TMB. No absorption peak at the long wavelength demonstrated the size, and morphology of SeNPs had no obvious changes after catalyzing the oxidation of TMB. Furthermore, no obvious change was observed in the UV–Vis absorption spectra of SeNPs before and after the reaction, confirming that the SeNPs worked as catalyst in the oxidation of TMB. Here, SeNPs used as mimic enzyme may accelerate the electrons transfer between the substrate TMB and dissolved oxygen.

Next, we studied the effects of pH, temperature, SeNPs concentration, and size on catalytic activity of the SeNPs.

Like natural enzyme, the activity of SeNPs was also dependent on pH and temperature. The curve and photograph of the oxidase-like activity of SeNPs under different pH are shown in Fig. 4a, from which can be seen that the optimum pH was 4.0. Figure 4b shows

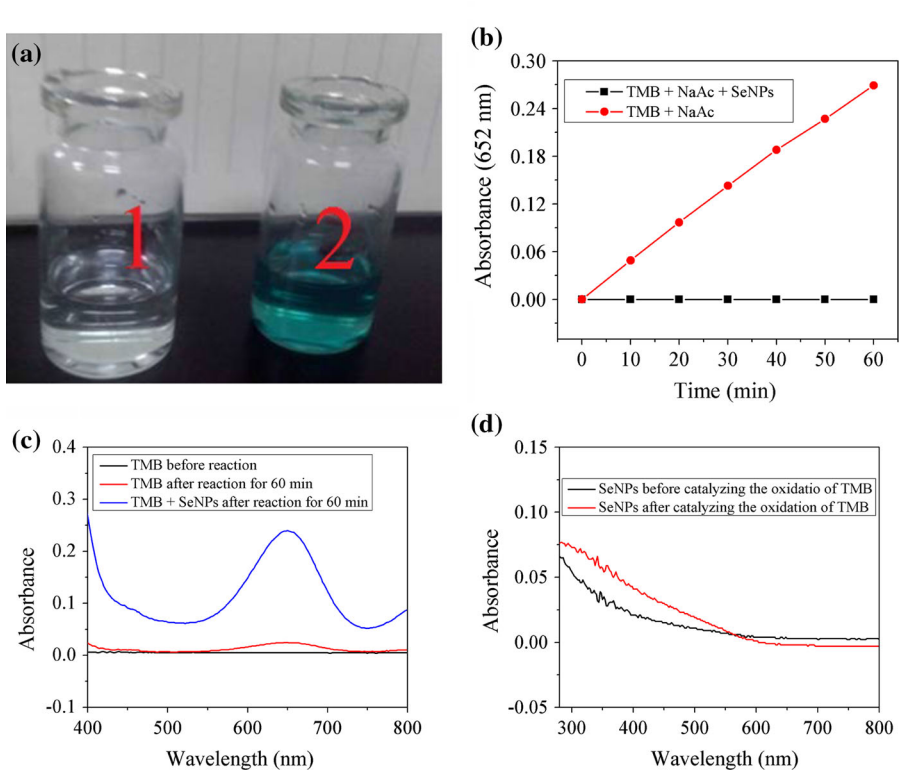

Fig. 3 **a** The color evolution of TMB oxidation in different reaction systems. *1* TMB + NaAc, *2* TMB + NaAc + SeNPs; **b** The absorbance of the oxidation products of TMB at 652 nm in the absence and presence of SeNPs (60 μg/mL); Experiment were carried out in a volume of 4 mL, 0.2 M NaAc buffer (pH 4.0), with 833 μmol/L TMB as substrate, reaction temperature 30 °C; **c** The UV–Vis absorption spectrum of TMB and the oxidation products of TMB with and without SeNPs; **d** The UV–Vis absorption spectrum of SeNPs before and after catalyzing the oxidation of TMB. (Color figure online)

the UV–Vis absorption spectrum of SeNPs after catalyzing the oxidation of TMB under different pH. The absorption spectrum of SeNPs in NaAc solution with different pH displayed no significant difference, which revealed that the pH did not affect the size and morphology of SeNPs. The pH-dependent activity of SeNPs may be attributed to the interaction between catalyst and substrate under different pH (Yang et al. 2013; Zhang et al. 2008). Temperature not only can alter the reaction speed, but also can affect the stability of the nanoparticles. Figure 4c shows the oxidase-like activity of SeNPs in the range of 20–60 °C. SeNPs exhibited high activity at the range of 25–35 °C and the optimum temperature was 30 °C. As the temperature was above 35 °C, the activity of the SeNPs decreased sharply. In order to reveal the relation between the structure of SeNPs and its temperature-dependent activity, the UV–Vis absorption spectrum of SeNPs after catalyzing the oxidation of TMB under different temperatures is shown in Fig. 4d. SeNPs displayed the similar absorption spectrum in the range of 20–35 °C, indicating that SeNPs maintained stability at low temperature. However, a remarkable absorption peak at ~540 nm was observed in the absorption spectrum of SeNPs as the temperature was above 35 °C. As previously reported, the peaks above 530 nm can be solely attributed to interchain interactions perpendicular to the c axis within a given t-Se crystal (Prabhu et al. 2013). The absorption spectrum exhibited a large red shift, which might be associated with the increased size and crystallization behaviors of SeNPs as the temperature was above 35 °C. Therefore, temperature affects the structure of SeNPs and its activity.

Previous works indicated that different sizes of SeNPs could be synthesized by changing the BSA concentration in the redox system. Generally, higher BSA concentration leads to smaller SeNPS size (Zhang et al. 2004). Here, SeNPs with mean diameters of 38.7 nm and 55.8 nm were obtained by adding 400 and 25 mg BSA into the redox system, respectively. As shown in Fig. 4f, the UV–Vis absorption spectrum of SeNPs was size-dependent. A remarkable absorption peak at 275 nm was observed in the absorption spectrum of SeNPs with larger diameter (55.8 nm), which was consistent with previous study (Yu et al.

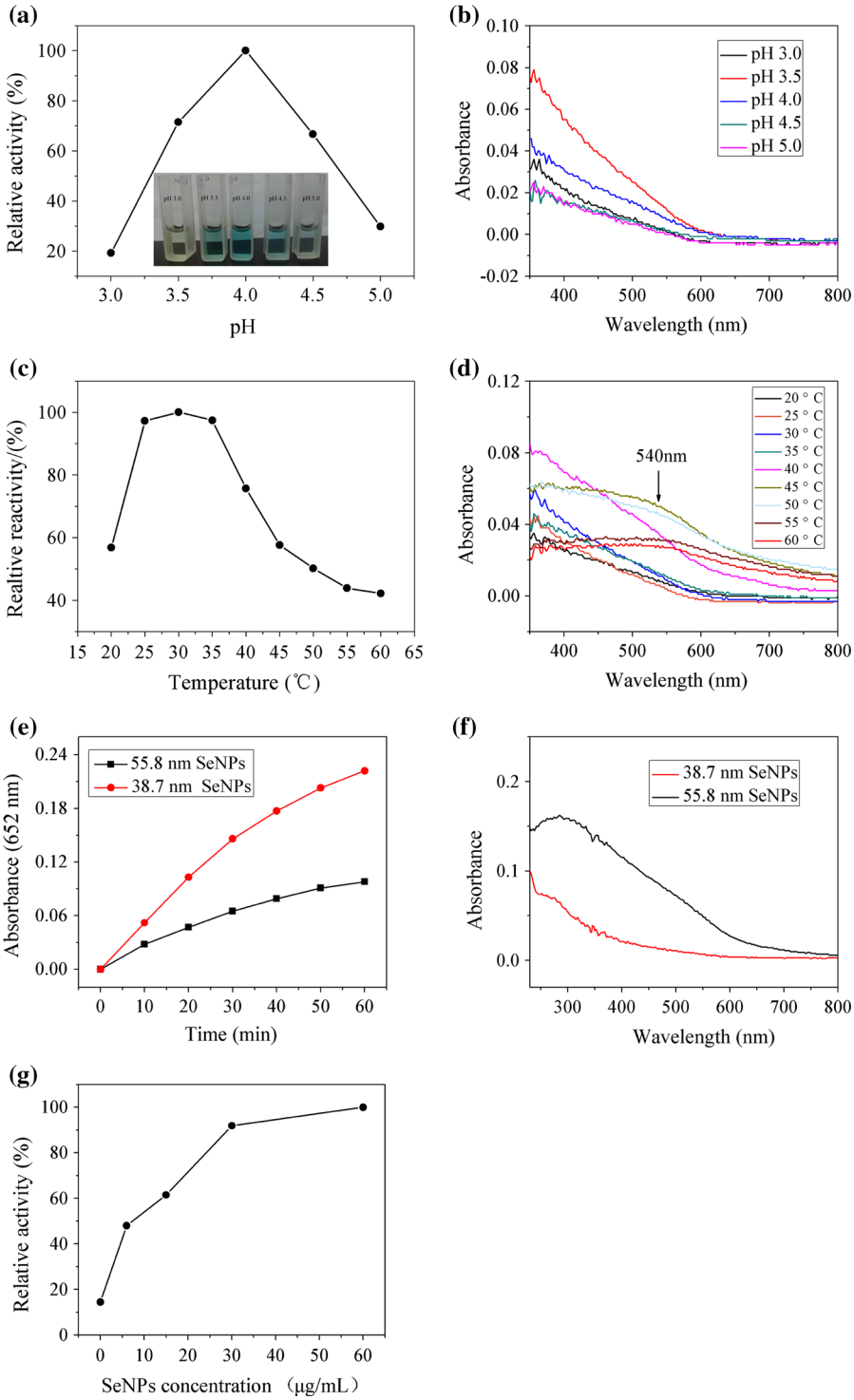

Fig. 4 **a** Effect of pH on the oxidase-like activity of SeNPs. TMB concentration: 833 μmol/L, SeNPs concentration: 60 μg/mL, reaction temperature 30 °C; **b** The UV–Vis absorption spectrum of SeNPs after catalyzing the oxidation of TMB under different pH; **c** Effect of temperature on the oxidase-like activity of SeNPs. TMB concentration: 833 uM, SeNPs concentration: 60 μg/mL, pH 4.0 NaAc buffer; **d** The UV–Vis absorption spectrum of SeNPs after catalyzing the oxidation of TMB under different temperatures; **e** Size dependence of the oxidase-like activity of SeNPs. TMB concentration: 833 μmol/L, SeNPs concentration: 60 μg/mL, pH 4.0 NaAc buffer, reaction temperature 30 °C; **f** The UV–Vis absorption spectrum of SeNPs with different sizes; **g** Effect of SeNPs concentration on its catalytic activity. TMB concentration: 833 μmol/L, pH 4.0, temperature 30 °C

2015). The catalytic activities of the two sizes SeNPs are shown in Fig. 4e; SeNPs with small size showed a higher catalytic activity compared to the large size SeNPs. Nanoparticles with small size can lead to large surface area which is important in the catalytic reaction. Here, small size SeNPs with well distribution

can provide enough surface area for the substrate and result in high catalytic activity.

Figure 4g shows the relationship between SeNPs concentration and its catalytic activity. It was found that the catalytic activity of SeNPs enhanced with the increase of SeNPs concentration. As SeNPs concentration remains in a relative low range (6–30 μg/mL), the relationship between the SeNPs concentration catalyst and catalytic activity is nearly linear. When SeNPs concentration increases to over 30 μg/mL and up to 60 μg/mL, the relationship between the SeNPs concentration and catalytic activity becomes sublinear and increasing slowly. When SeNPs concentration was relative low, which means the substrate was excess, the reaction speed depends on the concentration of SeNPs catalyst. As SeNPs concentration increases to a exceed range, the reaction speed depends not only on the concentration of SeNPs catalyst, but also on the substrate concentration. This causes the relationship between SeNPs concentration and catalytic activity to become sublinear.

Since SeNPs exhibited oxidase-like activity, the apparent steady-state kinetic parameters of TMB were obtained by varying TMB concentration. As shown in Fig. 5a, a typical Michaelis–Menten curve was obtained with TMB by recording the absorbance change at 652 nm for 60 min at an interval of 10 min. The Michaelis–Menten constant (K_m) and maximum initial velocity (V_{max}) were obtained using a Lineweaver–Burk plot. The values of K_m and V_{max} for the SeNPs with TMB were 0.0083 mol/L and 3.042 μmol/L min, respectively. K_m is an important parameter for measuring binding affinity of the enzyme to the substrates and affects the value of the reaction rate. A low K_m means the strong affinity of the enzyme to the substrates. As compared with other nanozyme, such as Fe_3O_4 nanoparticles, Pt nanoparticles, gold nanoparticles, and CuO nanoparticles, the K_m for the SeNPs with TMB was higher; meanwhile, the V_{max} for the SeNPs with TMB was lower (An et al. 2013; Shen et al. 2015; Tao et al. 2015). However, Se is an essential trace element of fundamental importance to human health, thus SeNPs have unique biocompatibility as compared with other nanozyme. The intrinsic oxidase-like activity of SeNPs provides a new molecular explanation for the biological function of SeNPs observed in cell and animal experiments. Furthermore, the intrinsic oxidase-like activity of SeNPs may expand the application area of element Se in biosensors, biochemistry detection, nanomedicine fields, and so on.

Conclusion

In conclusion, biocompatibility amorphous SeNPs with spherical morphology and a mean diameter of 38.7 nm were synthesized by the wet chemical reduction method using GSH as a reductant and BSA as a protective agent. The as-synthesized SeNPs can act as mimic oxidase and catalyze the oxidation reaction of substrate TMB producing a blue color product oxTMB. The influencing factors of the catalytic reaction were studied and the data showed that the optimal pH and temperature are approximately pH 4 and 30 °C, respectively. The size and

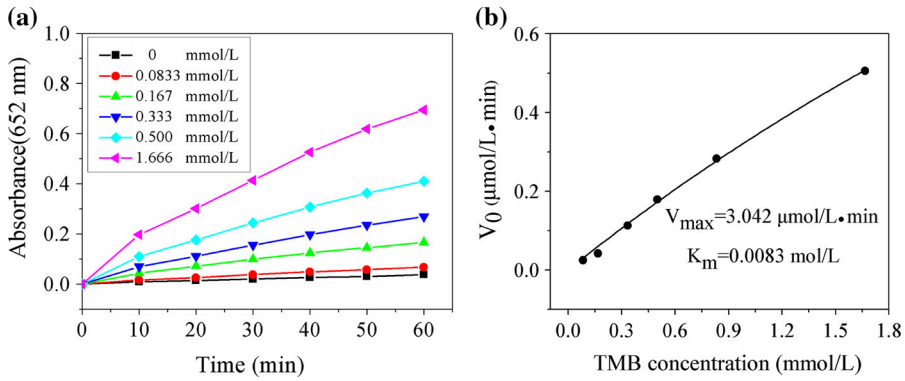

Fig. 5 **a** The time-dependent absorbance changes at 652 nm of various concentrations of TMB. SeNPs (38.7 nm) concentration: 60 μg/mL, pH 4.0 NaAc buffer, reaction temperature 30 °C; **b** The steady-state kinetic assay of SeNPs with TMB

concentration of the SeNPs also can affect their oxidase-like activity. The K_m and V_{max} of the SeNPs for TMB oxidation were 0.0083 mol/L and 3.042 μmol/L min, respectively. Although, the oxidase-like activity of SeNPs was lower than other nanostructures mimic enzyme as Fe_3O_4 nanoparticles, Pt nanoparticles, CuO nanoparticles etc., SeNPs with excellent biocompatibility which act as mimic enzyme were still of great significance. The oxidase-like activity of SeNPs may not only offer a new explanation for the high biological activity and low toxicity of SeNPs observed in cell and animal, but also can broaden the potential applications of selenium in biosensors, biochemistry detection, nanomedicine fields, and so on.

Acknowledgments We thank the faculty from Analytical and Testing Center of Huazhong University of Science and Technology. This work was supported by grants from the National Natural Science Foundation of China (Project No. 31170775)and the "Youth Chen-Guang Project" of Wuhan Bureau of Science and Technology (2015070404010184).

References

Abdulah R, Miyazaki K, Nakazawa M, Koyama H (2005) Chemical forms of selenium for cancer prevention. J Trace Elem Med Biol 19:141–150

An Q, Sun C, Li D, Xu K, Guo J, Wang C (2013) Peroxidase-like activity of Fe_3O_4@carbon nanoparticles enhances ascorbic acid-induced oxidative stress and selective damage to PC-3 prostate cancer cells. ACS Appl Mater Interfaces 5:13248–13257

Asati A, Kaittanis C, Santra S, Perez JM (2011) pH-tunable oxidase-like activity of cerium oxide nanoparticles achieving sensitive fluorigenic detection of cancer biomarkers at neutral pH. Anal Chem 83:2547–2553

Benko I et al (2012) Subacute toxicity of nano-selenium compared to other selenium species in mice. Environ Toxicol Chem 31:2812–2820

Dutta AK, Maji SK, Srivastava DN, Mondal A, Biswas P, Paul P, Adhikary B (2012) Synthesis of FeS and FeSe nanoparticles from a single source precursor: a study of their photocatalytic activity, peroxidase-like behavior, and electrochemical sensing of H_2O_2. ACS Appl Mater Interfaces 4:1919–1927

Feng Y, Su J, Zhao Z, Zheng W, Wu H, Zhang Y, Chen T (2014) Differential effects of amino acid surface decoration on the anticancer efficacy of selenium nanoparticles. Dalton Trans 43:1854–1861

Feng YB, Hong L, Liu AL, Chen WD, Li GW, Chen W, Xia XH (2015) High-efficiency catalytic degradation of phenol based on the peroxidase-like activity of cupric oxide nanoparticles. Int J Environ Sci Technol 12:653–660

Forootanfar H, Adeli-Sardou M, Nikkhoo M, Mehrabani M, Amir-Heidari B, Shahverdi AR, Shakibaie M (2014) Antioxidant and cytotoxic effect of biologically synthesized selenium nanoparticles in comparison to selenium dioxide. J Trace Elem Med Biol 28:75–79

Gao L et al (2007) Intrinsic peroxidase-like activity of ferromagnetic nanoparticles. Nat Nanotechnol 2:577–583

Gao F et al (2014) Cytotoxicity and therapeutic effect of irinotecan combined with selenium nanoparticles. Biomaterials 35:8854–8866

Gao L et al (2015) Peptide-conjugated gold nanoprobe: intrinsic nanozyme-linked immunsorbant assay of integrin expression level on cell membrane. ACS Nano 9:10979–10990

Hatfield DL, Tsuji PA, Carlson BA, Gladyshev VN (2014) Selenium and selenocysteine: roles in cancer, health, and development. Trends Biochem Sci 39:112–120

Hayat A, Cunningham J, Bulbul G, Andreescu S (2015) Evaluation of the oxidase like activity of nanoceria and its application in colorimetric assays. Anal Chim Acta 885:140–147

Huang B, Zhang J, Hou J, Chen C (2003) Free radical scavenging efficiency of Nano-Se in vitro. Free Radic Biol Med 35:805–813

Hunter WJ, Manter DK (2009) Reduction of selenite to elemental red selenium by Pseudomonas sp. Strain CA5. Curr Microbiol 58:493–498

Kumar A, Sevonkaev I, Goia DV (2014) Synthesis of selenium particles with various morphologies. J Colloid Interface Sci 416:119–123

Li H, Zhang J, Wang T, Luo W, Zhou Q, Jiang G (2008) Elemental selenium particles at nano-size (Nano-Se) are more toxic to Medaka (Oryzias latipes) as a consequence of hyper-accumulation of selenium: a comparison with sodium selenite. Aquat Toxicol 89:251–256

Lin Y, Ren J, Qu X (2014) Catalytically active nanomaterials: a promising candidate for artificial enzymes. Acc Chem Res 47:1097–1105

Peng D, Zhang J, Liu Q, Taylor EW (2007) Size effect of elemental selenium nanoparticles (Nano-Se) at supranutritional levels on selenium accumulation and glutathione S-transferase activity. J Inorg Biochem 101:1457–1463

Prabhu K, Mohanraj K, Kannan S, Barathan S, Sivakumar G (2013) Effect of pH, L-arginine concentration, and aging time on selenium nanostructures. Synth React Inorg Met Org Nano Met Chem 44:383–388

Shen X, Liu W, Gao X, Lu Z, Wu X, Gao X (2015) Mechanisms of oxidase and superoxide dismutation-like activities of gold, silver, platinum, and palladium, and their alloys: a general way to the activation of molecular oxygen. J Am Chem Soc 137:15882–15891

Tao Y, Ju E, Ren J, Qu X (2015) Bifunctionalized mesoporous silica-supported gold nanoparticles: intrinsic oxidase and peroxidase catalytic activities for antibacterial applications. Adv Mater 27:1097–1104

Vekariya KK, Kaur J, Tikoo K (2012) ERα signaling imparts chemotherapeutic selectivity to selenium nanoparticles in breast cancer. Nanomed Nanotechnol Biol Med 8:1125–1132

Wang H, Zhang J, Yu H (2007) Elemental selenium at nano size possesses lower toxicity without compromising the fundamental effect on selenoenzymes: comparison with

selenomethionine in mice. Free Radic Biol Med 42:1524–1533

Wang X, Sun K, Tan Y, Wu S, Zhang J (2014) Efficacy and safety of selenium nanoparticles administered intraperitoneally for the prevention of growth of cancer cells in the peritoneal cavity. Free Radic Biol Med 72:1–10

Wang Y, Chen P, Zhao G, Sun K, Li D, Wan X, Zhang J (2015) Inverse relationship between elemental selenium nanoparticle size and inhibition of cancer cell growth in vitro and in vivo. Food Chem Toxicol 85:71–77

Wei H, Wang E (2013) Nanomaterials with enzyme-like characteristics (nanozymes): next-generation artificial enzymes. Chem Soc Rev 42:6060–6093

Xu C, Lin Y, Wang J, Wu L, Wei W, Ren J, Qu X (2013) Nanoceria-triggered synergetic drug release based on CeO_2-capped mesoporous silica host-guest interactions and switchable enzymatic activity and cellular effects of CeO_2. Adv Healthc Mater 2:1591–1599

Yang M, Guan Y, Yang Y, Xia T, Xiong W, Wang N, Guo C (2013) Peroxidase-like activity of amino-functionalized magnetic nanoparticles and their applications in immunoassay. J Colloid Interface Sci 405:291–295

Yu S et al (2015) The inhibitory effect of selenium nanoparticles on protein glycation in vitro. Nanotechnology 26:145703–145717

Zhang J, Wang H, Bao Y, Zhang L (2004) Nano red elemental selenium has no size effect in the induction of seleno-enzymes in both cultured cells and mice. Life Sci 75:237–244

Zhang J et al (2008) Decomposing phenol by the hidden talent of ferromagnetic nanoparticles. Chemosphere 73:1524–1528

Zhang X, He S, Chen Z, Huang Y (2013) $CoFe_2O_4$ nanoparticles as oxidase mimic-mediated chemiluminescence of aqueous luminol for sulfite in white wines. J Agric Food Chem 61:840–847

Zheng W et al (2015) Multifunctional polyamidoamine-modified selenium nanoparticles dual-delivering siRNA and cisplatin to A549/DDP cells for reversal multidrug resistance. Acta Biomater 11:368–380